Materials and Methods

Human study participants

The study included 2 affected children from 2 distinct families. All probands were affected with recessive germline *DPP9* mutations (Fig. 1A). The study protocol was approved by A*STAR IRB (2019-087) and genetic analyses were performed in accordance with bioethics rules of national laws. Written informed consents were obtained from all the participants or their parents. The study was approved by and performed in accordance with the requirements of the institutional ethics committees of The Rockefeller University Hospital, New York, USA; Stanford University School of Medicine, Stanford, California, USA; and Necker-Enfants Malades Hospital, Paris, France. Informed consent was obtained for all patient and healthy control volunteers reported in the study.

DNA extraction, quantification, and quality control

Genomic DNA of the affected individuals and other available family members was extracted from either whole blood using a variety of extraction protocols. DNA concentration and quality were assessed using NanoDrop (Thermo Scientific) and Qubit (Life technologies) fluorometers. A260/A280 ratios of 1.8 to 2.0 and A260/A230 ratios >1.5 were accepted. DNA fragmentation was assessed using agarose gel (0.8%) electrophoresis.

Exome sequencing

Exome sequencing was employed independently for the detection of variants in Families 1 and 2.

Family 1 - Trio exome sequencing was performed using DNA extracted from peripheral blood samples at the Baylor Medical Genetics Laboratories according to published methods(*26*, *27*). Briefly, capture was performed with VCRome 2.1 in-solution exome probes, as well as additional probes for over 3,600 Mendelian-disease-related genes. Library DNA was sequenced on an Illumina HiSeq for 100 bp paired-end reads. Data analysis was performed with Mercury 1.0. Genes possibly associated with the patient's phenotype under a recessive mode of inheritance were reported in *DPP9*, *MS4A2*, *MXRA5* and *PAPLN*.

Family 2 - Genomic DNA (gDNA) was prepared from blood samples from patient II:1 by the standard phenol-chloroform extraction method. WES was performed with the SureSelect Human All Exon 71 Mb kit (Agilent Technologies). Paired-end sequencing was performed on a HiSeq 2500 machine (Illumina) generating 100-base reads. We aligned the sequences with the GRCh37 reference build of the human genome with the Burrows-Wheeler aligner(*28*). Downstream processing and variant calling were performed with the Genome Analysis Toolkit(*29*), SAMtools(*30*). Substitution and InDel calls were made with the GATK Unified Genotyper. All variants were annotated with annotation software developed in-house(*31–34*). Blacklisting variants common in private cohorts but not in public databases optimizes human exome analysis(*34*). Human Gene Mutation Database for any given gene(*35*). Based on the high consanguinity in this patient (1.66%), exome sequencing was analysed assuming autosomal recessive inheritance by keeping all homozygous non-synonymous coding variants and essential splice site variants with a MAF $<10^{-2}$ in different ethnic subpopulations.

Isolation of human fibroblasts and keratinocytes

Primary human fibroblasts and keratinocytes from Family 2 proband and two unaffected parental controls were isolated from fresh skin biopsies. Briefly, biopsies were incubated in dispase overnight at 4°C to enable peeling of the epidermis from the dermal compartment. Keratinocytes from the epidermis were then isolated by mechanical disruption and grown on

a 3T3 feeder layer. Fibroblasts were isolated by finely chopping up the dermis and incubating it overnight in collagenase D. The collagenase was then removed the next day and fibroblasts were allowed to migrate out of the dermal fragments.

Cell culture
All 293T lines and derivatives were cultured in DMEM supplemented with 10% FBS. Any control primary fibroblasts or keratinocytes used as WT controls were obtained from the Skin Research Institute of Singapore (SRIS) Skin Cell Bank with informed consent and prior IRB approval.

SDS PAGE western blot and ELISA
Protein lysate was quantified using Bradford assay and 20 ug of protein loaded unless stated otherwise. Western blotting was carried out by incubating the primary antibodies overnight in 3% Milk in TBST. All ELISA experiments were carried out according to manufacturer's instructions.

Luminex multiplex microbead-based immunoassay
Conditioned supernatants were collected for Luminex analysis using the ProcartaPlex, Human Customized 65-plex Panel (Thermo Fisher Scientific,) to measure the following targets: APRIL; BAFF; BLC; CD30; CD40L; ENA-78; Eotaxin; Eotaxin-2; Eotaxin-3; FGF-2; Fractalkine; G-CSF; GM-CSF; Gro a; HGF; IFN-a; IFN-g; IL-10; IL-12p70; IL-13; IL-15; IL-16; IL-17 A; IL-18; IL-1 A; IL-1 b; IL-2; IL-20; IL-21; IL-22; IL-23; IL-27; IL-2 R; IL-3; IL-31; IL-4; IL-5; IL-6; IL-7; IL-8; IL-9; IP-10; I-TAC; LIF; MCP-1; MCP-2; MCP-3; M-CSF; MDC; MIF; MIG; MIP1a; MIP-1 b; MIP-3 A; MMP-1; NGF beta; SCF; SDF-1 A; TNF b; TNF-a; TNF-R2; TRAIL; TSLP; TWEAK; VEGF-A.

Harvested supernatants and standards were incubated with fluorescent-coded magnetic beads pre-coated with respective antibodies in a black 96-well clear-bottom plate overnight at 4˚C. After incubation, plates were washed 5 times with wash buffer (PBS with 1% BSA (Capricorn Scientific) and 0.05% Tween-20 (Promega)). Sample-antibody-bead complexes were incubated with Biotinylated detection antibodies for 1 hour and washed 5 times with wash buffer. Subsequently, Streptavidin-PE was added and incubated for another 30 mins. Plates were washed 5 times again, before sample-antibody-bead complexes were re-suspended in sheath fluid for acquisition on the FLEXMAP® 3D (Luminex) using xPONENT® 4.0 (Luminex) software. Data analysis was done on Bio-Plex Manager™ 6.1.1 (Bio-Rad). Standard curves were generated with a 5-PL (5-parameter logistic) algorithm, reporting values for both mean fluorescence intensity (MFI) and concentration data. Hierarchical clustering and generation of heatmap was performed using pheatmap package on RStudio 1.3.1093.

Mice
DPP9$^{S729A/S729A}$ mice were provided by Prof Mark Gorrell (Centenary Institute). Nlrp1$^{-/-}$ (*36*), Gsdmd$^{-/-}$ (*37*), Ilr-1$^{-/-}$ (*38*), Asc$^{-/-}$ (*39*), Il-18$^{-/-}$ (*40*) were generated on, or backcrossed at least 10 generations onto the C57BL/6 background. Experiments use littermate controls where possible. All animal experiments complied with the regulatory standards of, and were approved by, the Walter and Eliza Hall Institute Animal Ethics Committee.

Histology
Organs were collected in 10% neutral buffered formalin. Organ sections were prepared from paraffin blocks and stained with hematoxylin and eosin. Immunohistochemistry was

performed using antibodies against F4/80 (in house), B220 (in house) or CD3 (Agilent #A045229).

Micro-CT
For Micro-CT scans mice were euthanised and scanned on a Bruker Skyskan 1276 Micro-CT. Images were analysed using Amaris software.

Hematology
Automated cell counts were performed on blood collected from the sub-mandibular vein into Microtainer tubes containing EDTA (Sarstedt), using an Advia2120i hematological analyser (Siemens, Munich, Germany).

FACs analysis of newborn pup blood and bone marrow
Pups were euthanised 3-6 hours after birth via decapitation and blood collected from the neck into Microtainer tubes containing EDTA (Sarstedt). Limbs and sternum were collected, bones were crushed and passed through a 40 uM filter to obtain a single cell suspension. $1x10^6$ cells of the bone suspension and 15 uL of blood were plated per sample before red cell depletion using RCR Buffer (156 mM NH_4Cl, 11.9 mM $NaHCO_3$, 0.097 mM EDTA). Cells were washed in PBS and incubated with rat anti-mouse CD16/CD23 (1:200 BioLegend #101302) at 4°C for 10 minutes to block Fc receptors. Cells were washed and stained for 1 hour at 4°C with fluorescently tagged antibodies: MHCII-FITC (1:200 in house), CD11c-PE (1:200 BioLegend #117307), CD4-PE-Cy7 (1:200 BioLegend #100528), CD3-PE-CF594 (1:200 BD Bioscience #562286), Ly6G-APC (1:200 in house), CD19-AF700 (1:200 BioLegend #15528), NK1.1-BV450 (1:400 BioLegend #108731), Zombie aqua viability Dye (1:500 Biolegend #77143), CD11b-BV605 (1:400 Biolegend 101257), CD8-BV650 (1:400 BioLegend #100742), Ly6C-BV711 (1:400 Biolegend #128037), CD45-BV786 (1:200 BioLegend #103149). Cells were washed and fixed with BD Phosflow Lyse/Fix buffer (BD Bioscience) for 20 min at RT and then stored at 4°C. Flow cytometry was performed on the BD LSRFortessa X-20 (BD Bioscience) and data acquired using BD FACSDiva (BD Bioscience) software. Data was analysed using FloJo (Tree Star). Gating strategy was as follows: $Ly6C^{med}$ and $Ly6C^{high}$ monocytes, $Ly6C^{med\ or\ hi}$, $CD11b^+$) dendritic cells ($CD11b^+$, $CD11c^+$, $MHCII^+$) T cells ($CD3^+$, $CD4^+$ or $CD8^+$), B cells ($CD19^+$, $CD3^-$), NK cells ($NK1.1^+$, $CD3^-$), and neutrophils ($Ly6G^+$, $CD11b^+$, Ly6C).

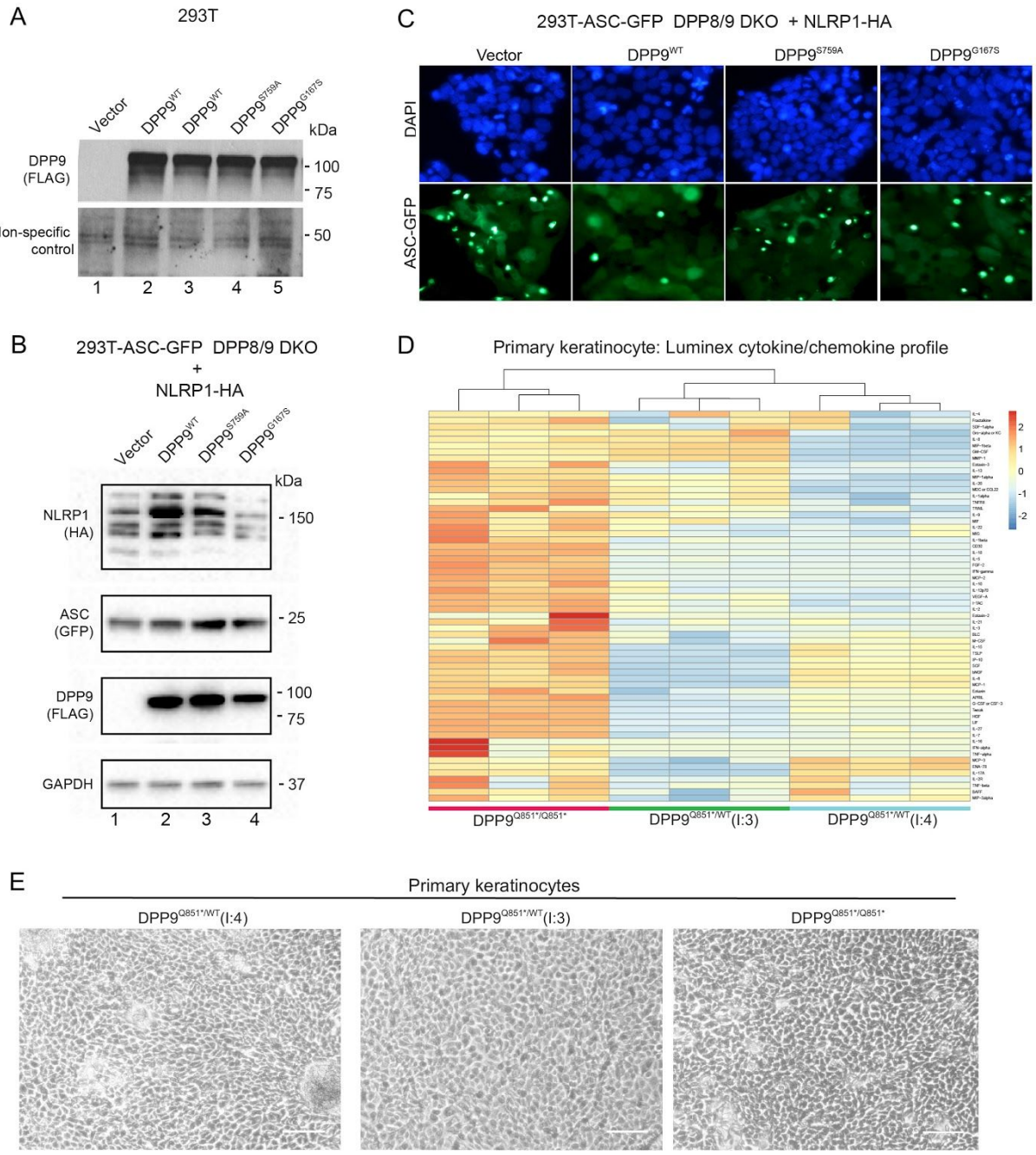

Figure S1: Mutant DPP9 alleles fail to inhibit NLRP1, eliciting release of proinflammatory cytokines

(A) DPP8/9 enzyme assay shows a reduction in DPP8/9-derived enzymatic activity in DPP9 S759A and G167S mutants. Western blot analysis of DPP9 protein levels or a non-specific loading control for data obtained in figure 2B.

(B) DPP9 S759A and G167S mutants are unable to repress NLRP1 inflammasome. Western blot analysis for NLRP1-HA, ASC-GFP and FLAG-DPP9, to confirm their expression in DPP8/9 DKO cells used in figure 2C.

(C) DPP9 S759A and G167S mutants are unable to repress NLRP1 inflammasome. 293T-ASC-GFP DPP8/9 DKO cells were transfected with a vector control or WT NLRP1 together with wild-type DPP9, DPP9 S759A, or DPP9 G167S. Figure shows representative images of percentage of cells with ASC-GFP specks for each transfected sample.

(D) Heatmap depicting Luminex cytokine/chemokine analysis and hierarchical clustering of primary keratinocyte cultures derived from proband and heterozygous parents of family 2.

(E) Primary keratinocytes isolated from the family 2 proband (II:3) are morphologically indistinguishable from the unaffected parents. Phase contrast images of primary keratinocytes from the two unaffected parents from family 2 ((I:2) and (I:1) (Q851X/+) and affected individual from family 2 (proband II:3; Q851X/Q851X).

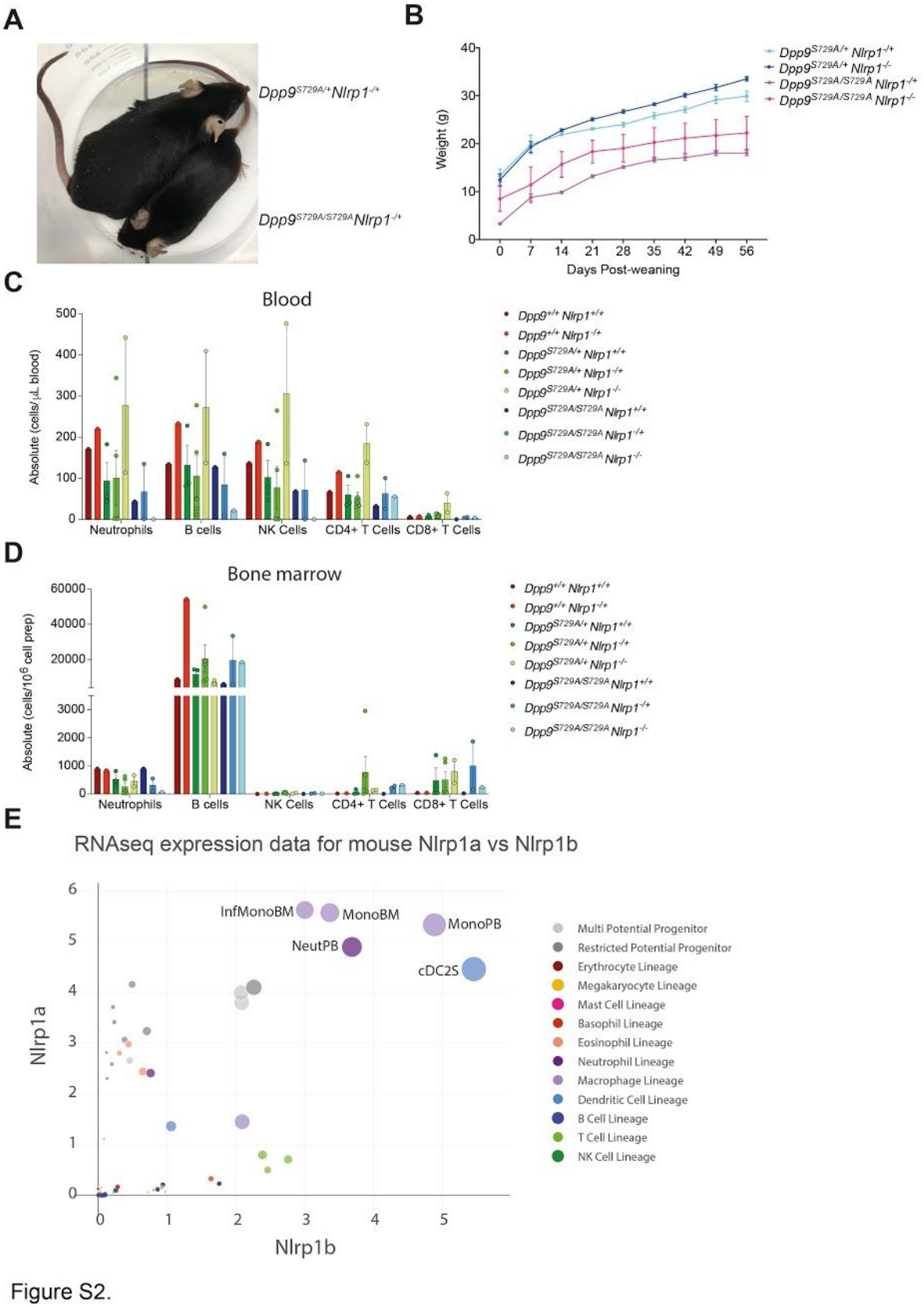
A
Dpp9S729A/+ Nlrp1-/+
Dpp9S729A/S729A Nlrp1-/+
B
Weight (g)
Days Post-weaning
Dpp9S729A/+ Nlrp1-/+
Dpp9S729A/+ Nlrp1-/-
Dpp9S729A/S729A Nlrp1-/+
Dpp9S729A/S729A Nlrp1-/-
C
Blood
Absolute (cells/μL blood)
Neutrophils
B cells
NK Cells
CD4+ T Cells
CD8+ T Cells
Dpp9+/+ Nlrp1+/+
Dpp9+/+ Nlrp1-/+
Dpp9S729A/+ Nlrp1+/+
Dpp9S729A/+ Nlrp1-/+
Dpp9S729A/+ Nlrp1-/-
Dpp9S729A/S729A Nlrp1+/+
Dpp9S729A/S729A Nlrp1-/+
Dpp9S729A/S729A Nlrp1-/-
D
Bone marrow
Absolute (cells/10^6 cell prep)
Neutrophils
B cells
NK Cells
CD4+ T Cells
CD8+ T Cells
E
RNAseq expression data for mouse Nlrp1a vs Nlrp1b
Nlrp1a
Nlrp1b
InfMonoBM
MonoBM
MonoPB
NeutPB
cDC2S
Multi Potential Progenitor
Restricted Potential Progenitor
Erythrocyte Lineage
Megakaryocyte Lineage
Mast Cell Lineage
Basophil Lineage
Eosinophil Lineage
Neutrophil Lineage
Macrophage Lineage
Dendritic Cell Lineage
B Cell Lineage
T Cell Lineage
NK Cell Lineage

Figure S2.

Figure S2: Heterozygous loss of NLRP1 rescues neonatal lethality of *Dpp9*$^{S729A/S729A}$ mice.
(A) A viable, male *Dpp9*$^{S729A/S729A}$ *Nlrp1*$^{-/+}$ mouse is runted compared to a *Dpp9*$^{S729A/+}$ *Nlrp1*$^{-/+}$ littermate.
(B) *Dpp9*$^{S729A/S729A}$ *Nlrp1*$^{+/-}$ mice exhibit stunted weight gain compared to *Dpp9*$^{S729A/+}$ *Nlrp1*$^{+/-}$ controls. Male *Dpp9*$^{S729A/S729A}$ *Nlrp1*$^{-/+}$ and *Dpp9*$^{S729A/+}$ *Nlrp1*$^{-/+}$ mice were weighed weekly for 8 weeks post weaning (n=2-5 per genotype).
(C) Neutrophils, NK cells, B cells and T cells numbers remain unchanged in newborn *Dpp9*$^{S729A/S729A}$ mice. FACs analysis of immune cells of the blood and (D) bone marrow collected from 3-6 hour-old pups.
(E) Expression of *Nlrp1a* and *Nlrp1b* is increased in monocytes and dendritic cell subsets compared to other lineages. RNA-seq expression data of *Nlrp1a* vs *Nlrp1b* in haematopoietic cell types.

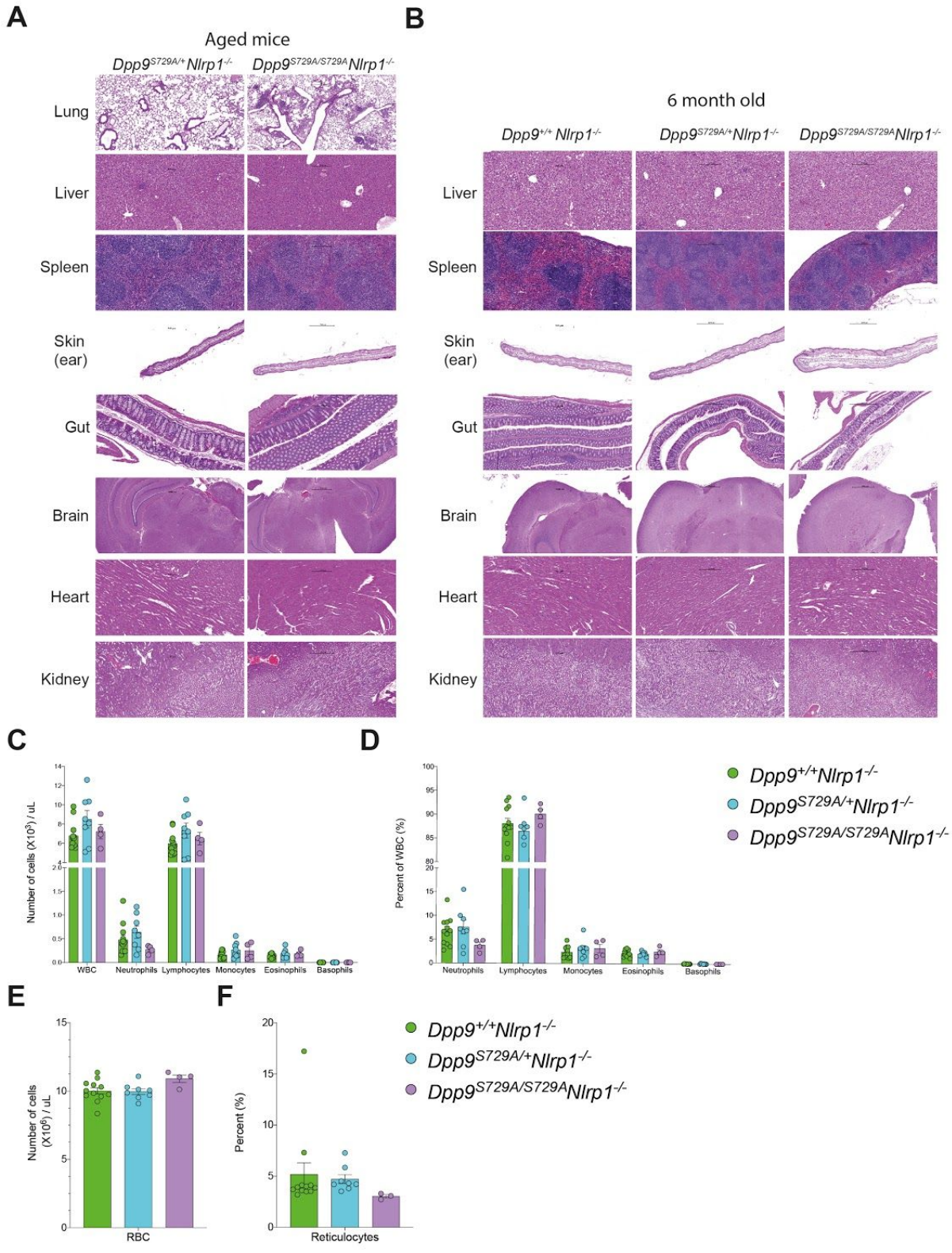

Figure S3.

Figure S3: *Dpp9*$^{S729A/S729A}$ *Nlrp1*$^{-/-}$ mice display accumulation of immune cell infiltrate in the lung

(A) *Dpp9*$^{S729A/S729A}$ *Nlrp1*$^{-/-}$ display immune cell infiltrate in lungs. Hematoxylin and eosin stained section of lung, liver, spleen, sternum, skin, gut, brain, heart and kidney tissue from

aged and (B) 6-month-old *Dpp9*$^{S729A/S729A}$ *Nlrp1*$^{-/-}$ and *Dpp9*$^{S729A/+}$ *Nlrp1*$^{-/-}$ mice. Black arrows indicate immune cell infiltrate. N=3-7 per genotype.
(C-F) Peripheral blood cell numbers remain unchanged in adult (4-months-old) *Dpp9*$^{S729A/S729A}$ *Nlrp1*$^{-/-}$ mice compared to controls. (C) Absolute and (D) percent of neutrophils, lymphocytes, monocytes, eosinophils and basophils. (E) Absolute number of red blood cells. (F) Percent of reticulocytes.

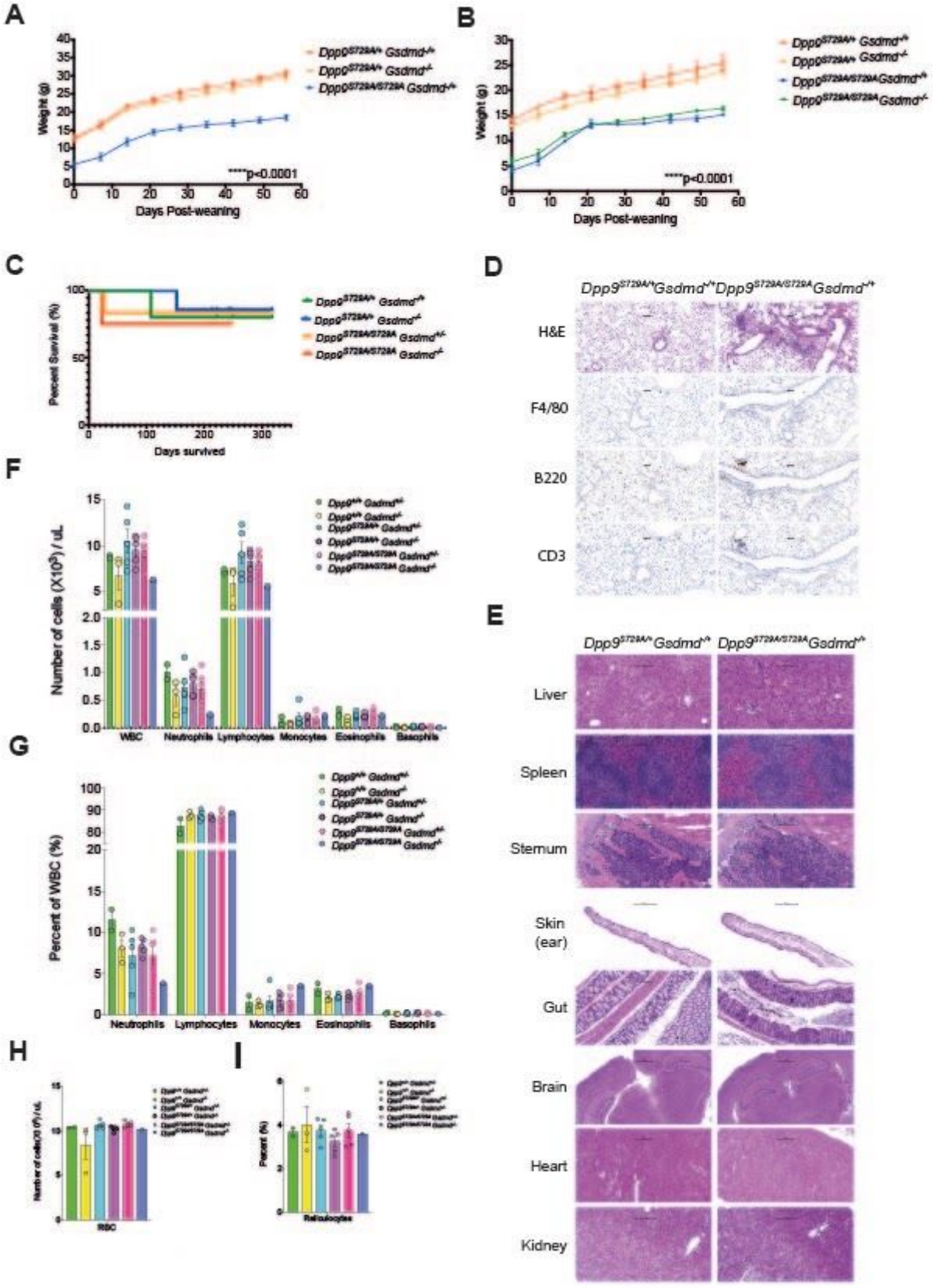

Figure S4: *Dpp9*$^{S729A/S729A}$ *Gsdmd*$^{-/-}$ mice phenocopy *Dpp9*$^{S729A/S729A}$ *Nlrp1*$^{-/-}$ mice.
(A) Male and (B) female *Dpp9*$^{S729A/S729A}$ deficient in GSDMD are runted compared to *Dpp9*$^{S729A/+}$ mice deficient in GSDMD. Mice were weighed weekly for 8 weeks post weaning to quantify the size difference.

(C) Post-weaning Kaplan Meier survival curve of *Dpp9*$^{S729A/S729A}$ or *Dpp9*$^{S729A/+}$ mice deficient in GSDMD showing no difference in survival up to 300 days.
(D) *Dpp9*$^{S729A/S729A}$ *Gsdmd*$^{-/+}$ mice display immune infiltrate in the lungs.
Immunohistochemistry of F4/80, B220 or CD3 antibodies on sections of mouse lung and (E) hematoxylin and eosin stained and on section of lung, liver, spleen, sternum, skin, gut, brain, heart and kidney tissue from 6-month-old *Dpp9*$^{S729A/S729A}$ *Gsdmd*$^{-/+}$ and *Dpp9*$^{S729A/+}$ *Gsdmd*$^{-/+}$ mice (n=2-4 per genotype).
(F-I) Peripheral blood cell numbers remain unchanged in adult (4-months-old) *Dpp9*$^{S729A/S729A}$ *Gsdmd*$^{-/-}$ mice compared to controls (F) Absolute and (G) percent of neutrophils, lymphocytes, monocytes, eosinophils and basophils. (H) Absolute number of red blood cells. (I) Percent of reticulocytes. Error bars represent mean ±SEM. Statistical significance was determined by one-way ANOVA.